

Supporting Information

Stacked CdTe/CdS Nanodiscs via Intraparticle Migration of CdTe on CdS

Seokpyo Jeon^{†,‡}, Taekyung Kim^{†,‡}, Jongsik Park^{†,||}, Taehyun Kwon[†], Hionsuck Baik[⊥], and
Kwangyeol Lee^{*,†}

[†] Department of Chemistry and Research Institute for Natural Sciences, Korea University, Seoul 02841, Korea

^{||} Department of Chemistry, Kyonggi University, Suwon 16227, Republic of Korea.

[⊥] Korea Basic Science Institute (KBSI), Seoul 02841, Korea

[‡] These authors contributed equally.

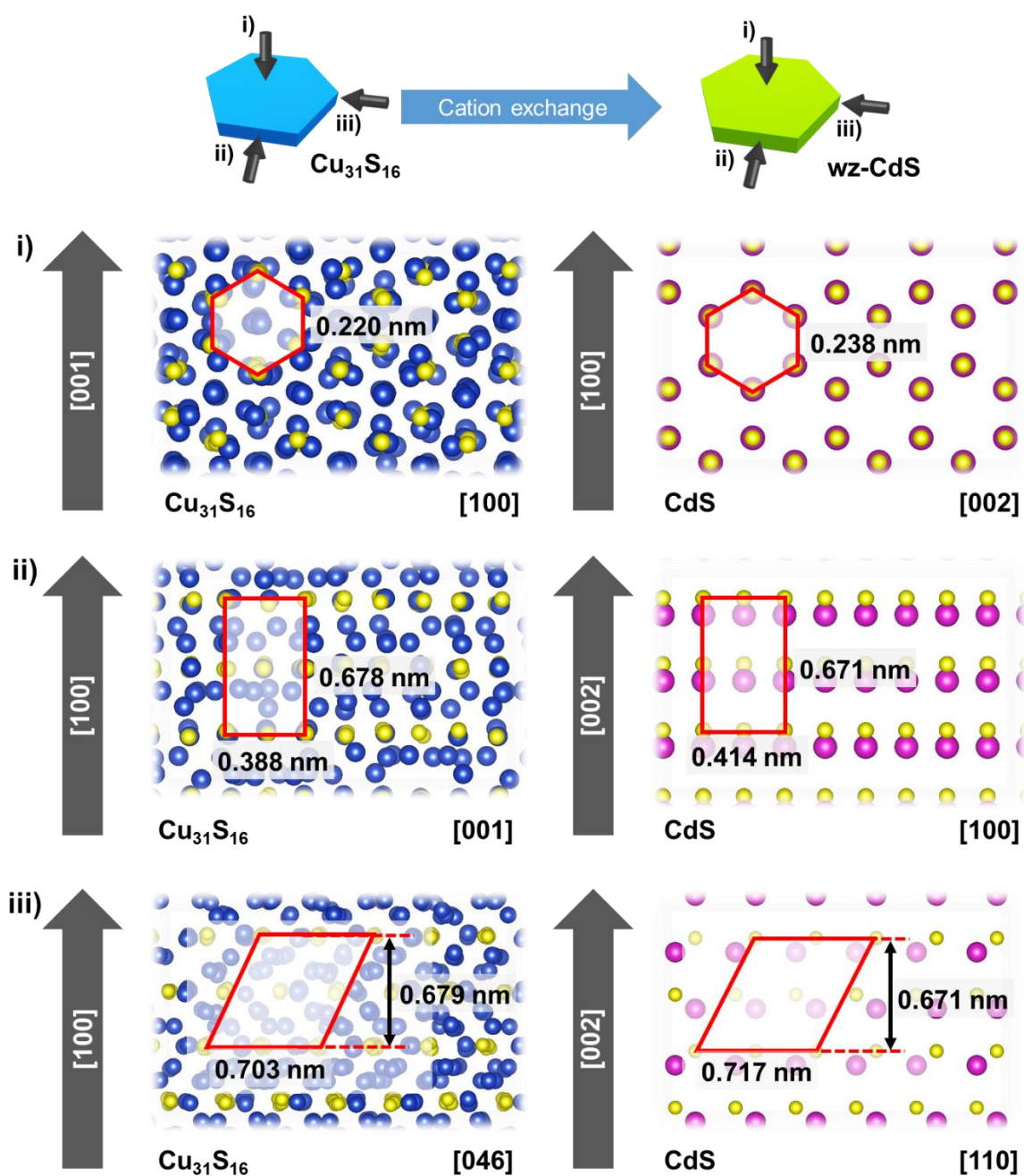


Figure S1. Crystal structures of $\text{Cu}_{31}\text{S}_{16}$ (CS) nanodisc (left column) and wz-CdS nanodisc (right column). Blue, magenta, and yellow colors indicate Cu, Cd, and S, respectively.¹

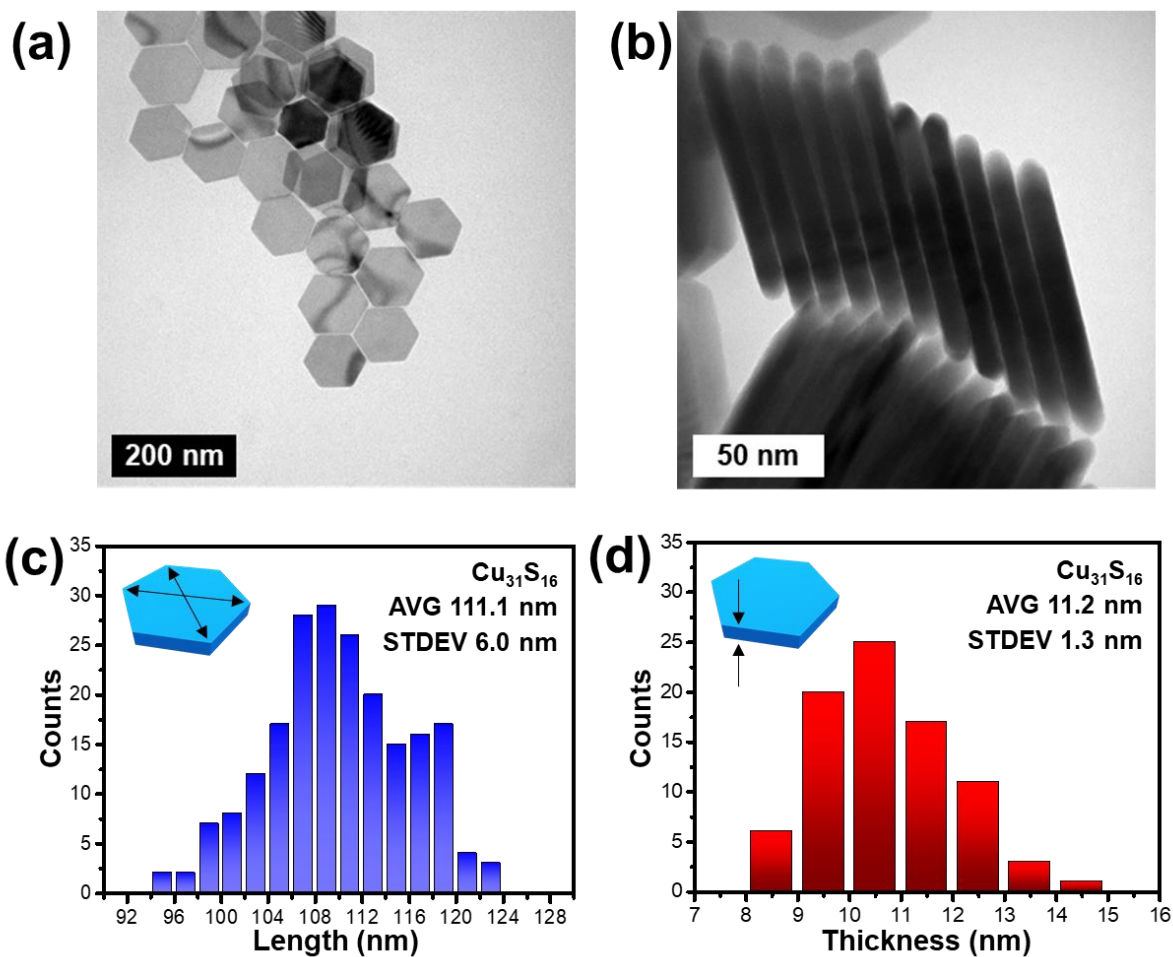


Figure S2. (a, b) TEM images and (c, d) the length and thickness distributions of $\text{Cu}_{31}\text{S}_{16}$ (CS) nanodiscs.

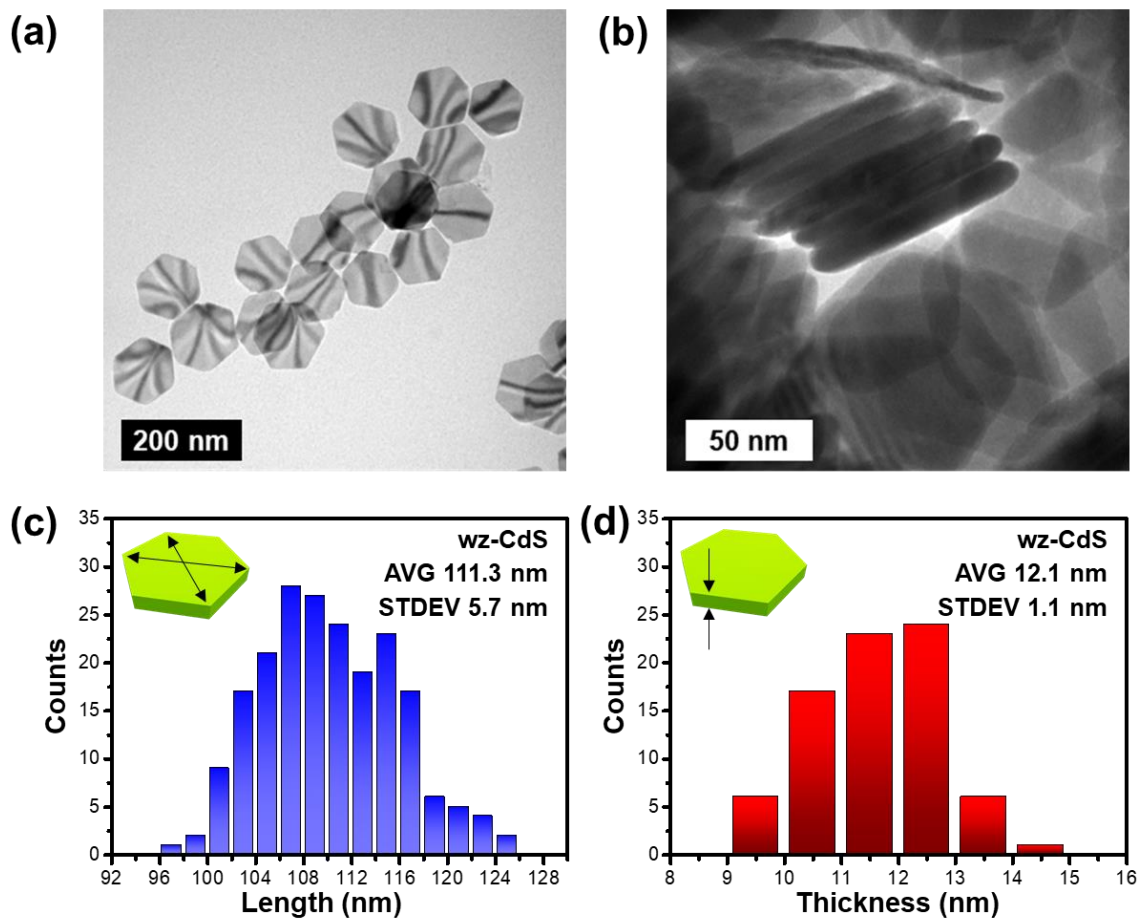


Figure S3. (a, b) TEM images and (c, d) the length and thickness distributions of wz-CdS nanodiscs.

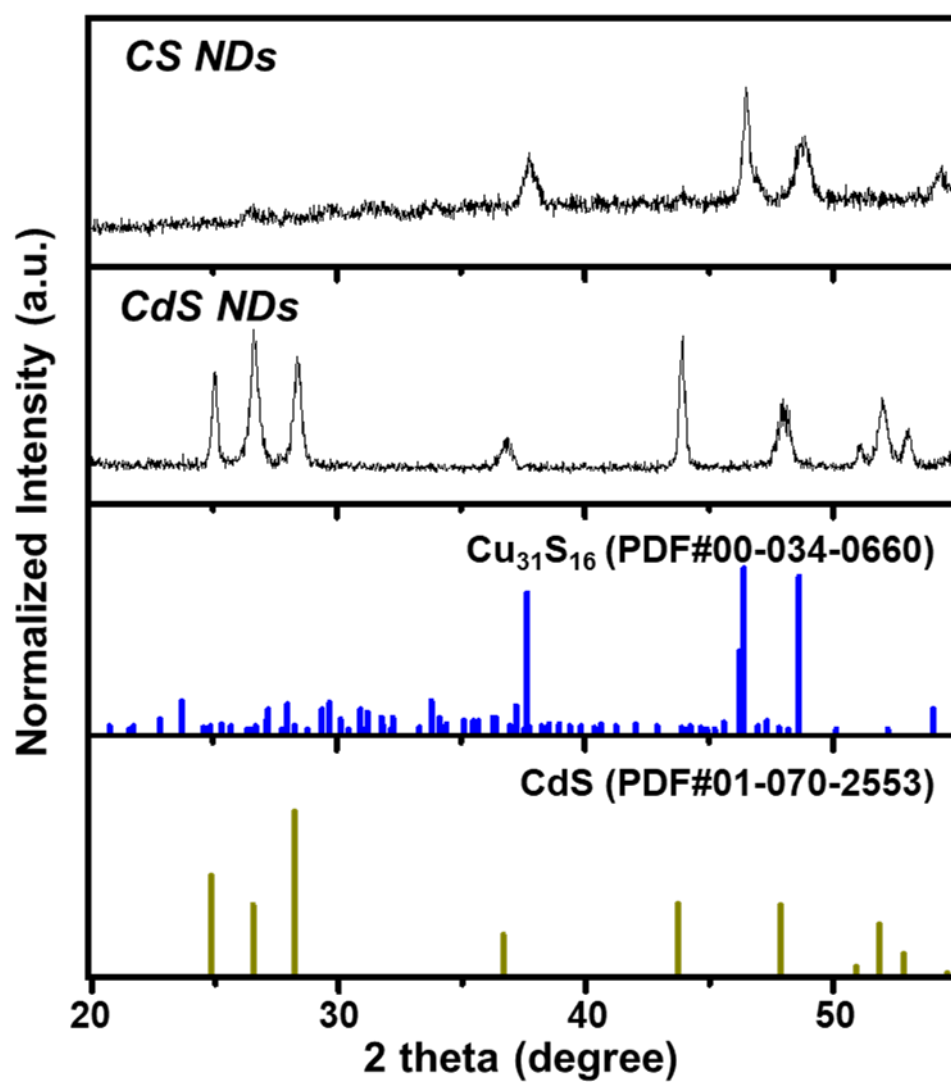


Figure S4. The XRD patterns of Cu₃₁S₁₆ (CS) nanodiscs and wz-CdS seeds.

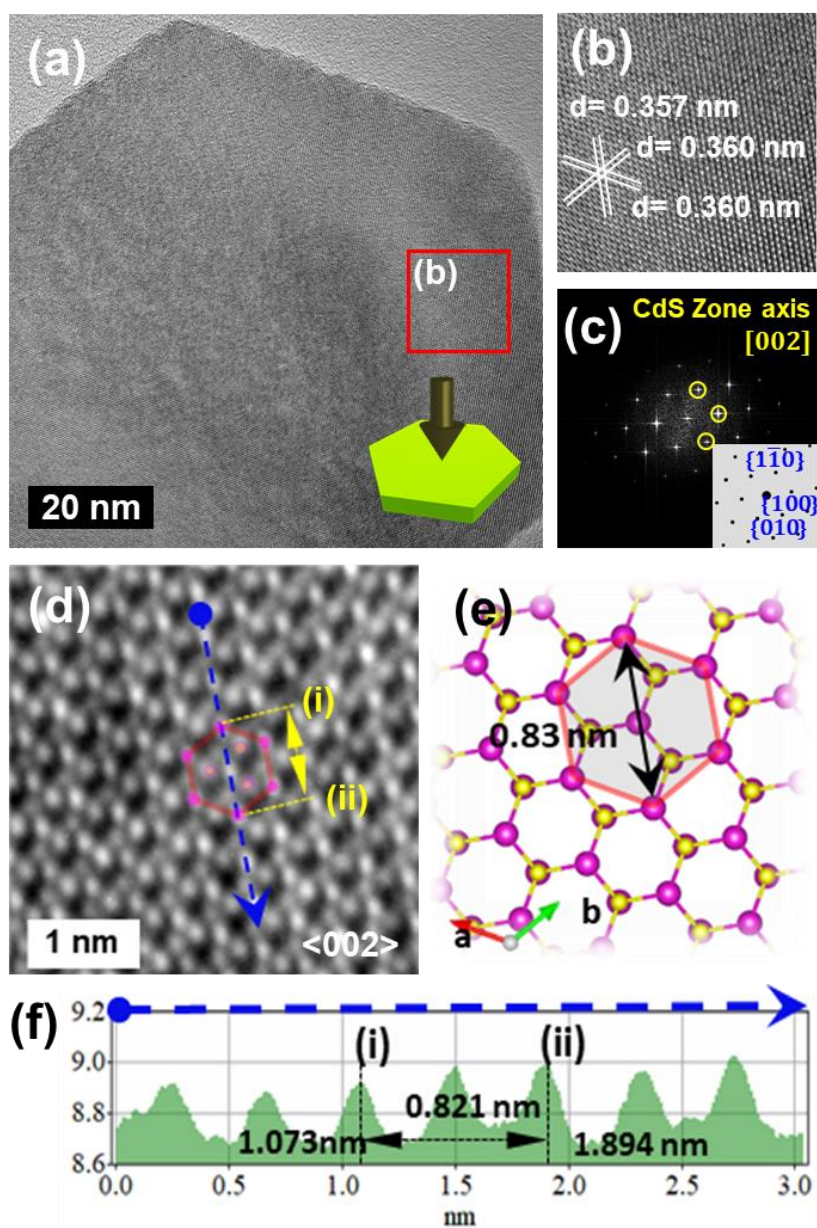


Figure S5. The characterization of CdS hexagonal seeds. (a) HRTEM image, (b) enlarged HRTEM image of CdS seed along the CdS [002], and (c) corresponding FFT pattern and simulated FFT pattern. (d) enlarged HRTEM image of CdS seed and (e) the corresponding atomic orientation. (f) Line profile analysis along the blue arrow direction in (d). Magenta and yellow colors indicate Cd and S, respectively.

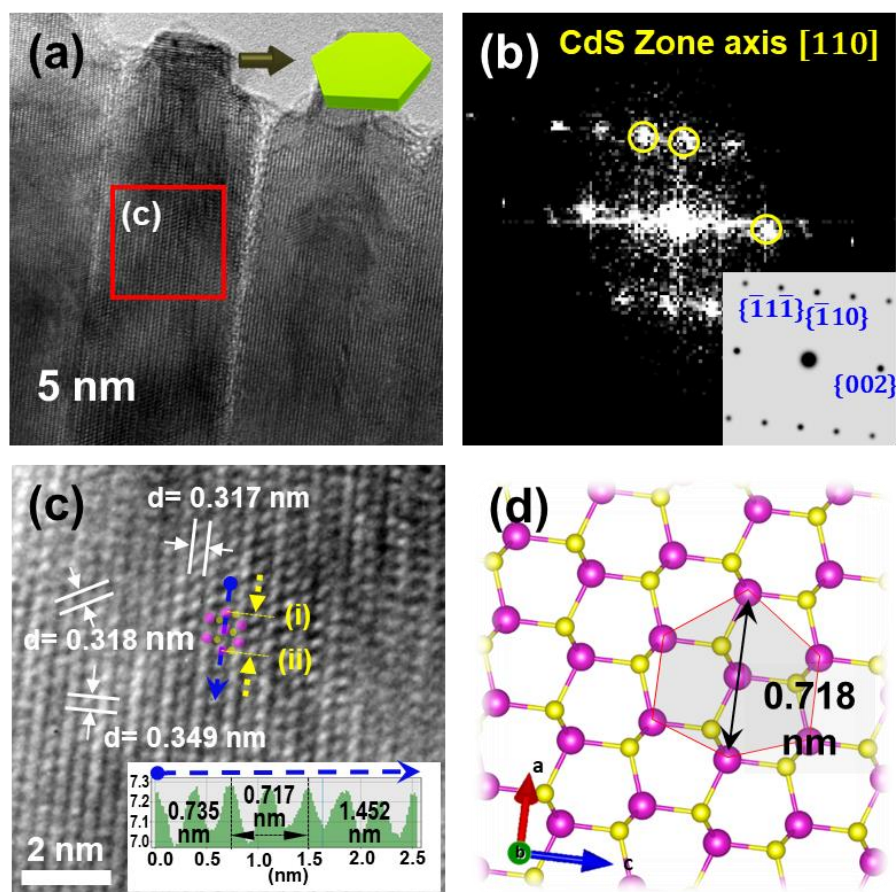


Figure S6. The characterization of CdS seeds from side view. (a) HRTEM image of CdS seed from CdS [110] and (b) corresponding FFT pattern of region (c) in (a) and simulated FFT pattern(inset). (c) Enlarged HRTEM image of CdS seed and corresponding line profile analysis along the blue dotted arrow direction and (d) corresponding atomic orientation of (c). Magenta and yellow colors indicate Cd and S, respectively.

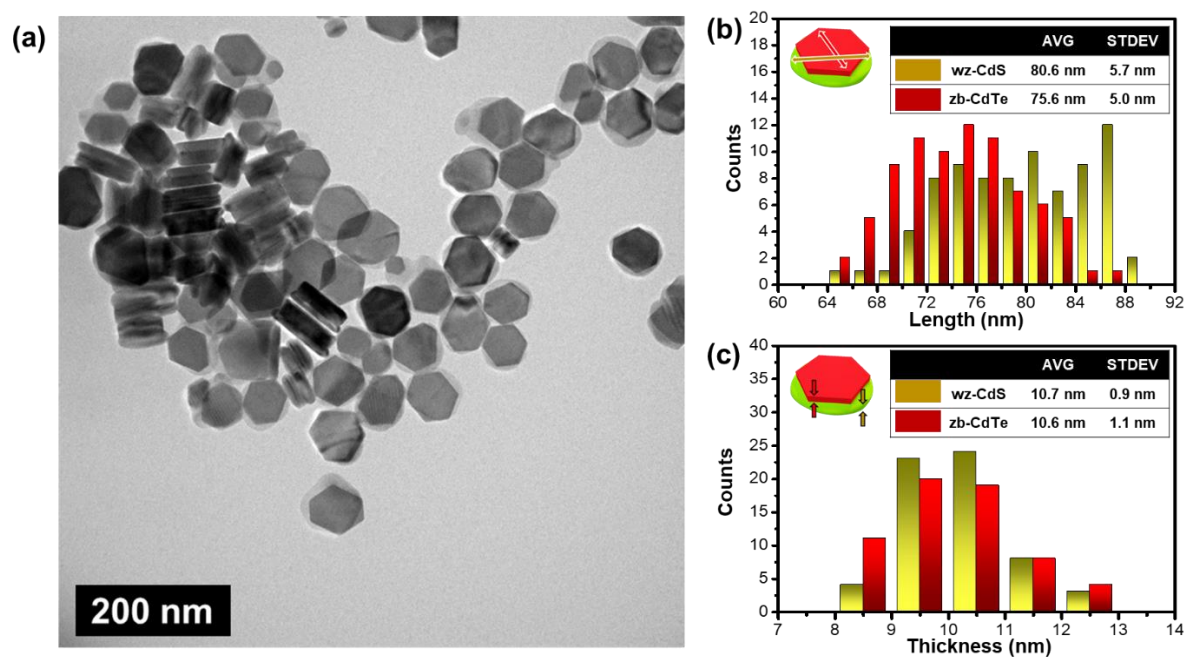


Figure S7. (a) TEM image, (b) the length, and (c) thickness distributions of stacked wz-CdS/zb-CdTe heteronanodiscs (s-CdST HNDs).

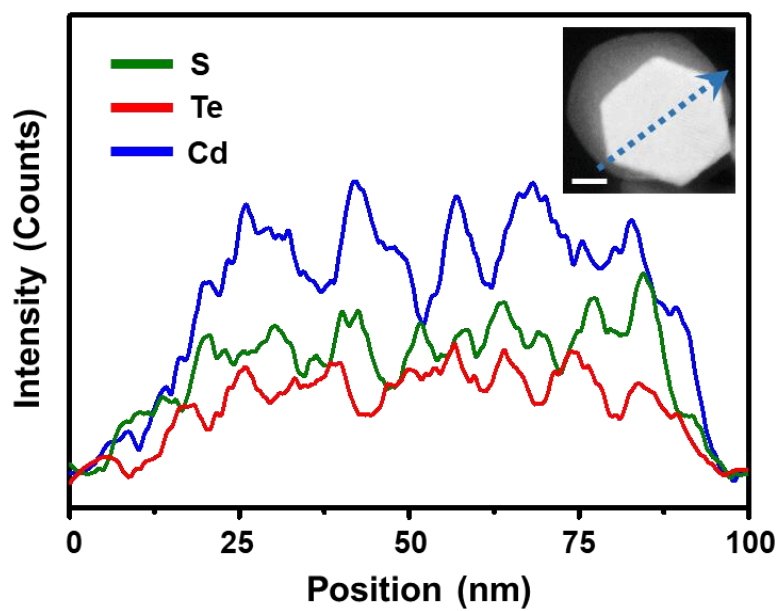


Figure S8. Line profile analysis of stacked wz-CdS/zb-CdTe heteronanodiscs (s-CdST HNDs) along the direction perpendicular to CdS [002]. Scale bar of inset HAADF-STEM image is 20 nm.

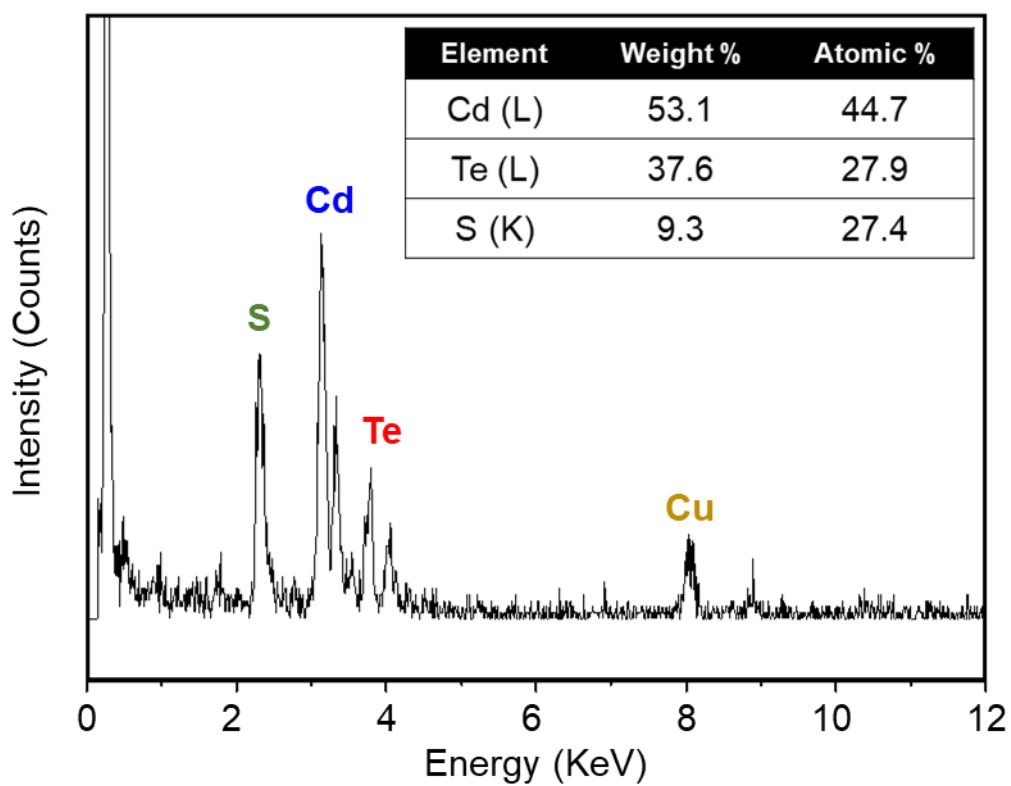


Figure S9. EDS spectra of stacked wz-CdS/zb-CdTe heteronanodiscs (s-CdST HNDs). The yellow Cu peak was caused by the TEM holder used for the TEM analysis.

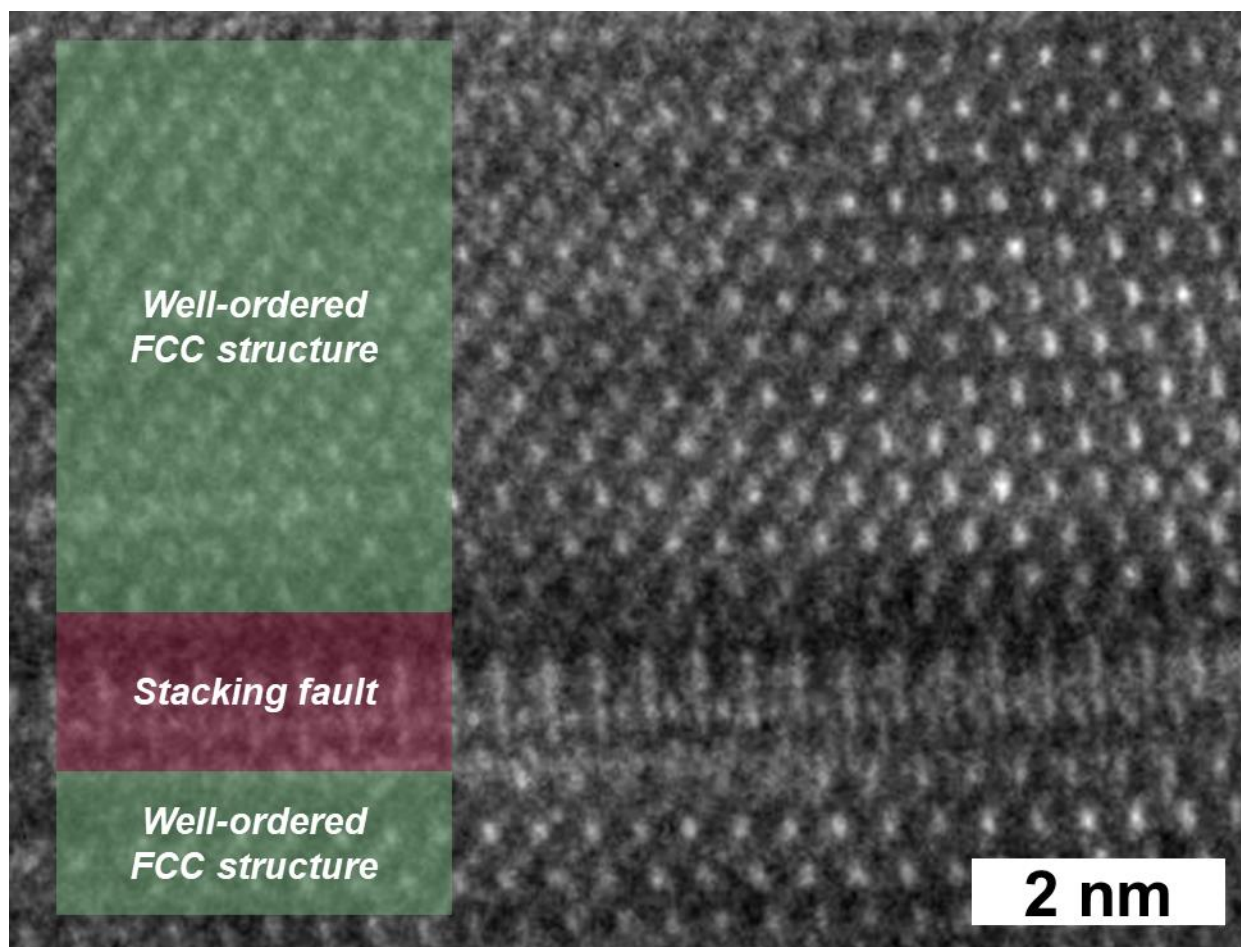


Figure S10. Enlarged HRTEM image of zb-CdTe region in Figure 2g which shows stacking fault in zb-CdTe structure.

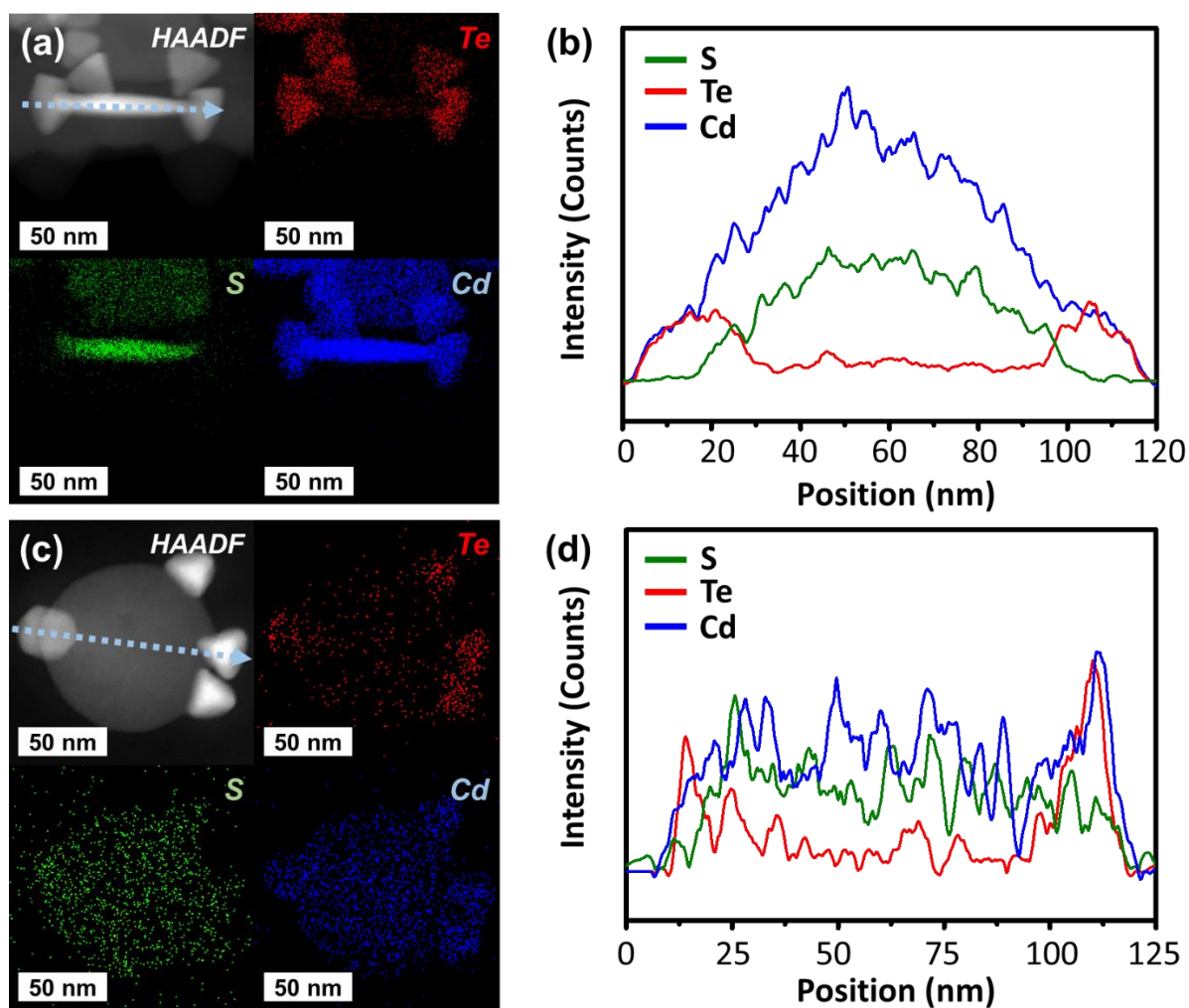


Figure S11. (a, c) HAADF-STEM and elemental mapping images of intermediate of s-CdST HND at 30 min from the side view and at 1 h from the top view, respectively and (b, d) corresponding line profile analysis along the direction of light blue dotted arrows in HAADF-STEM image of (a, c).

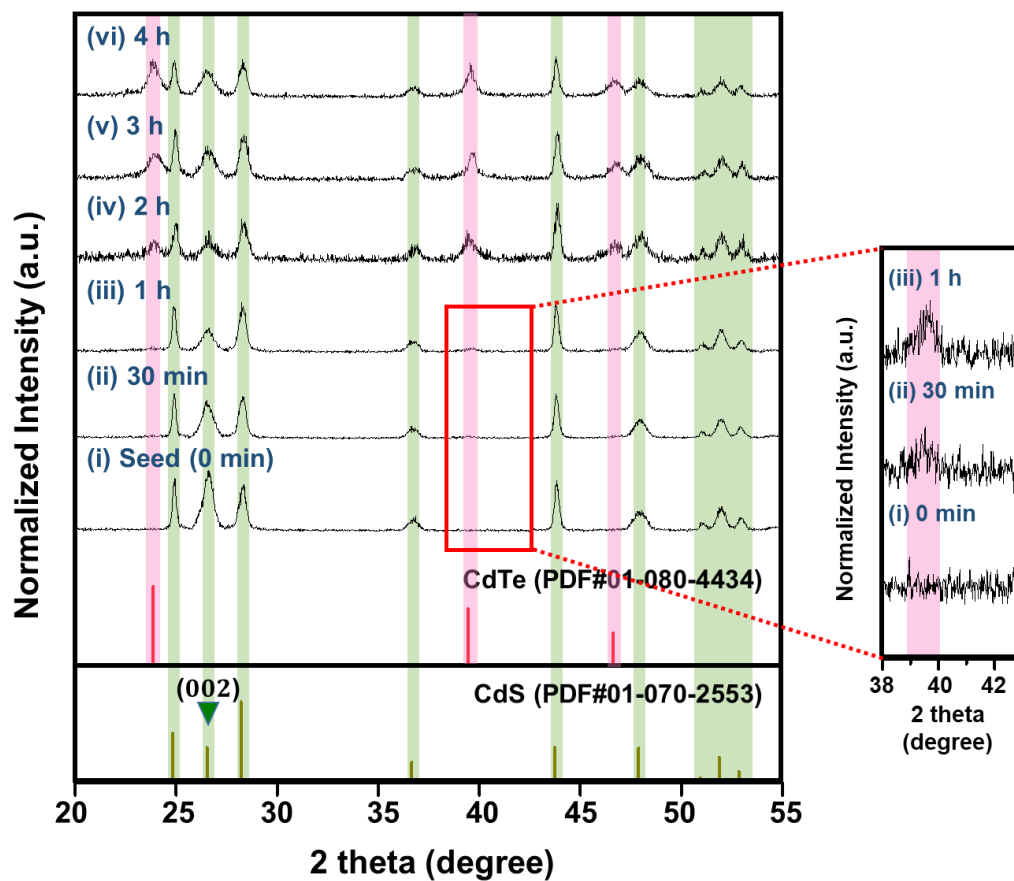


Figure S12. XRD patterns of reaction intermediates of s-CdST HNDs obtained from (a) 0 min, (b) 30 min, (c) 1 h, (d) 2 h, (e) 3 h and (d) 4 h.

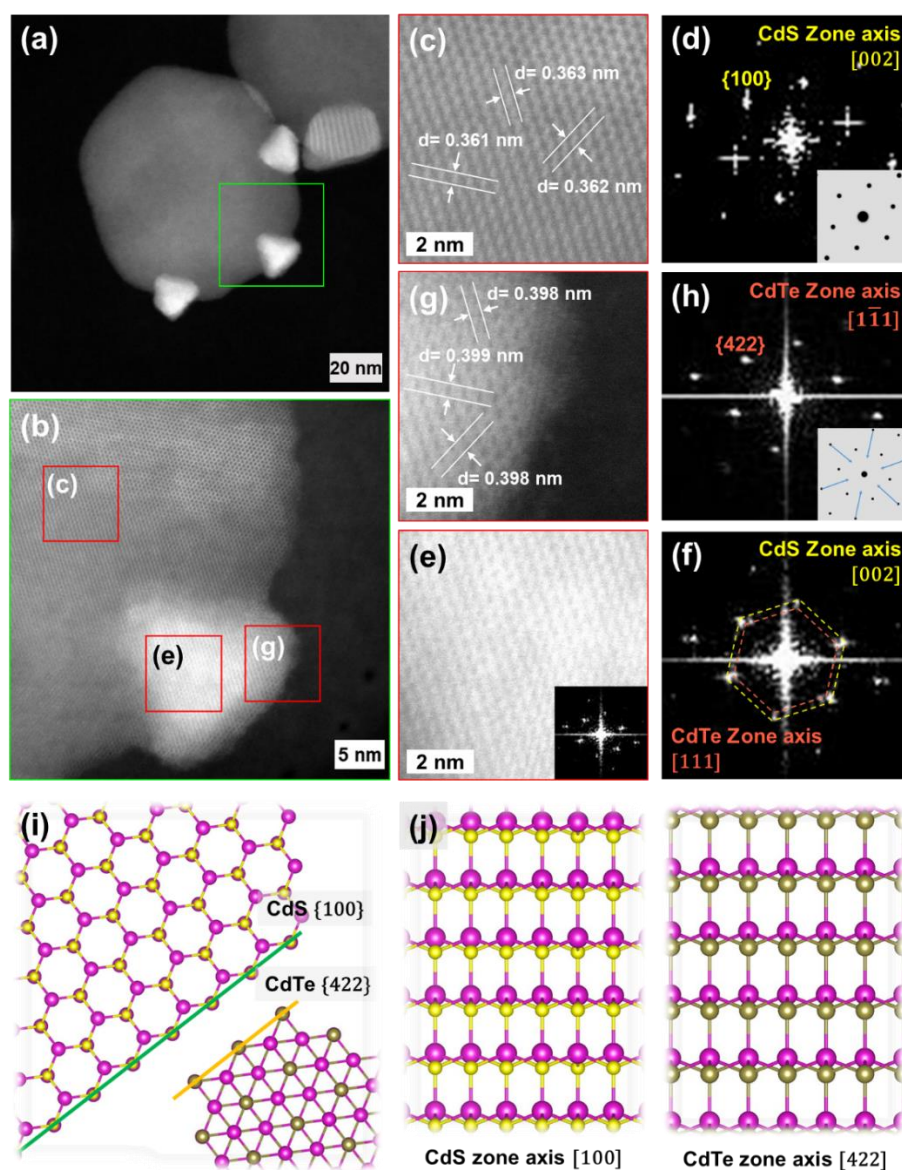


Figure S13. The characterization of s-CdST HNDs intermediate at 30 min. (a) HAADF-STEM image, (b) atomic-resolution HAADF-STEM image of green square in (a). (c, g, and e) Enlarged images of red squares in (b) and (d, h, and f) corresponding FFT patterns and simulated FFT patterns of wz-CdS, zb-CdTe, and stacked wz-CdS/zb-CdTe areas, respectively. Atomic orientations of s-CdST HNDs intermediate at 30 min (i) along the zone axes of CdS [002] and CdTe [$\bar{1}\bar{1}1$] and (j) zone axes of CdS [100] and CdTe [422].

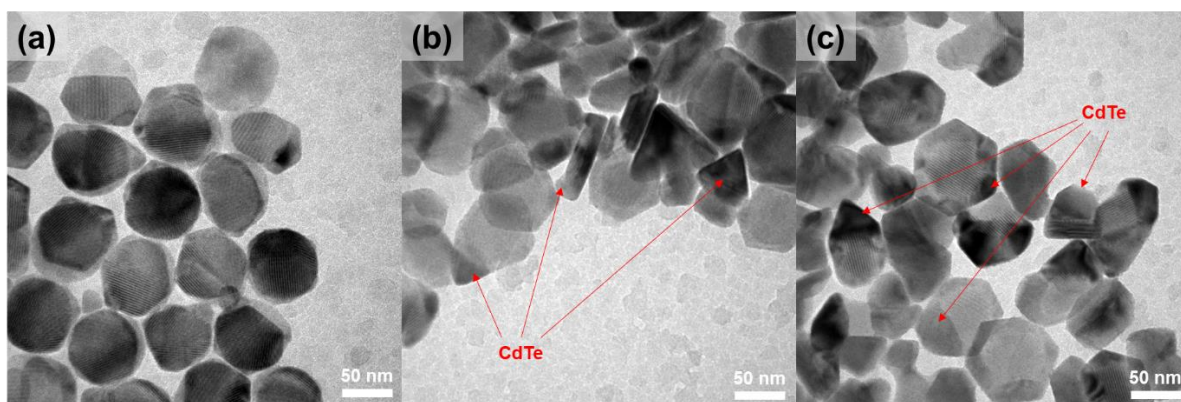


Figure S14. TEM images of s-CdST HNDs with varying reaction times obtained at (a) 4 h, (b) 6 h, and (c) 8 h.

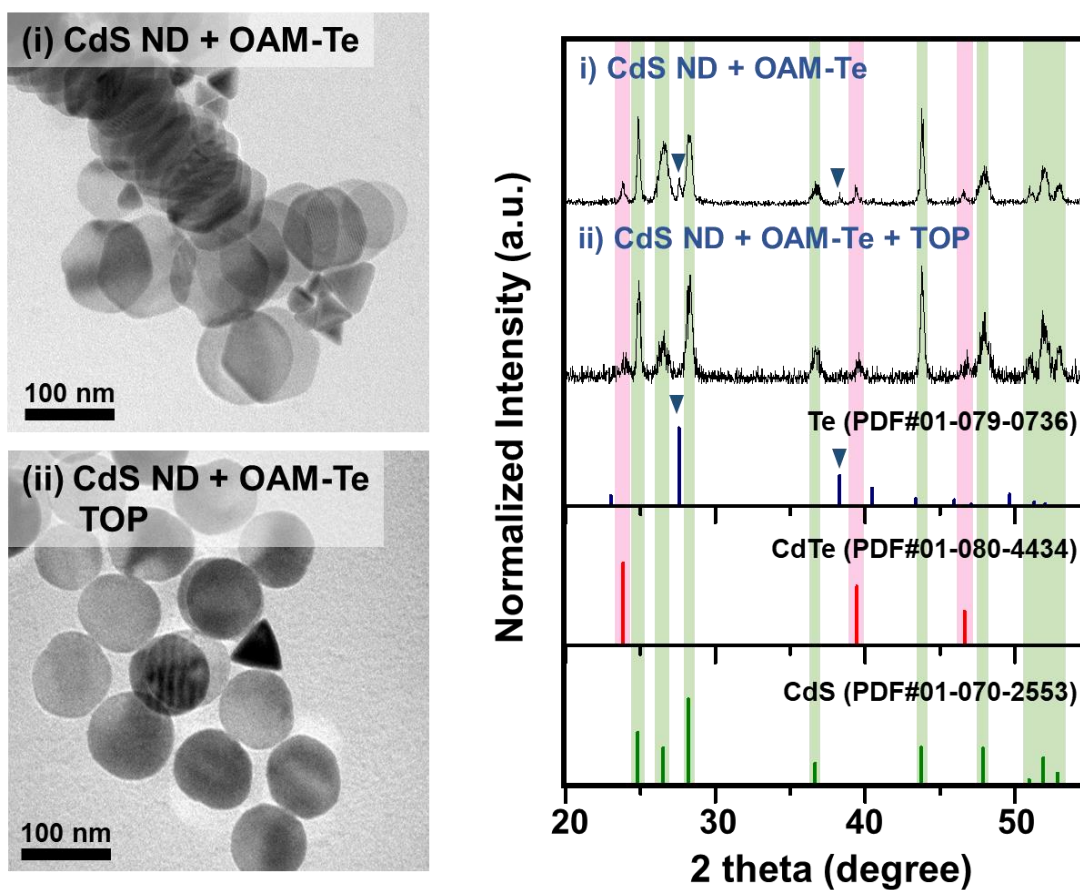


Figure S15. TEM images and XRD analysis of CdS ND reacted with OAM-Te and OAM-Te + TOP. The inversed triangles marked peaks on XRD pattern is corresponded by undissolved Te powder.

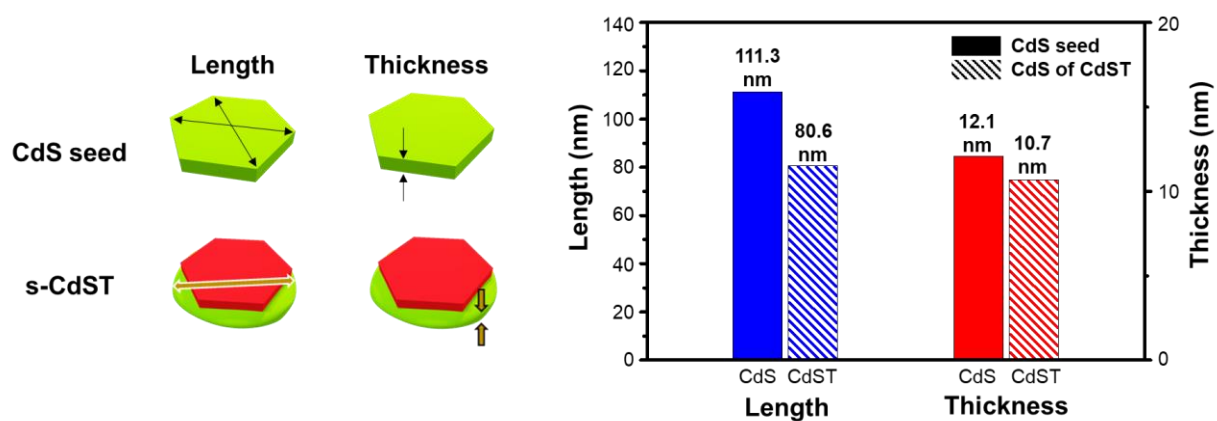


Figure S16. Comparison of overall dimension between CdS hexagonal plates and s-CdST HNDs.

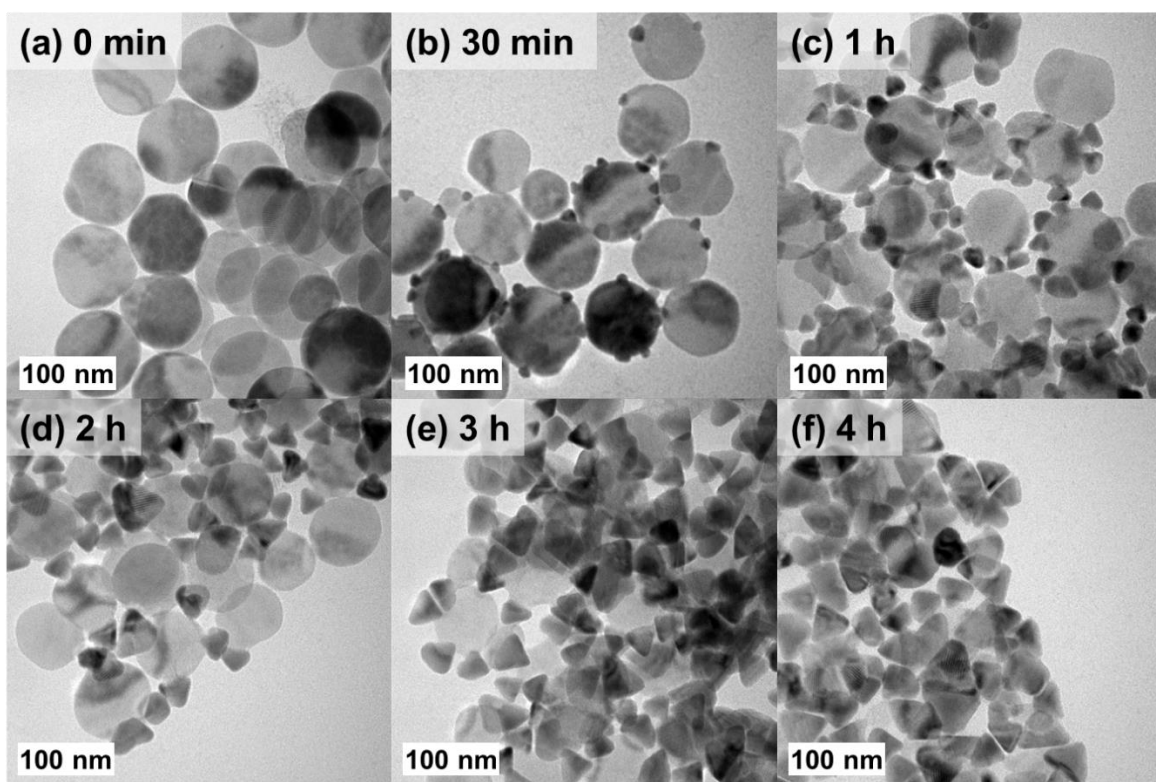


Figure S17. TEM images of intermediates obtained with varying reaction times of s-CdST HNDs at 280°C from (a) 0 min, (b) 30 min, (c) 1 h, (d) 2 h, (e) 3 h, and (f) 4 h.

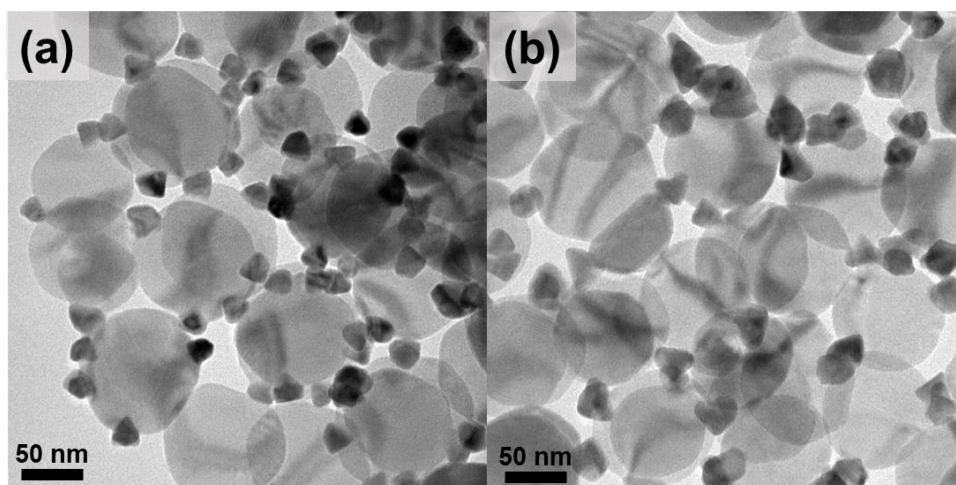


Figure S18. The TEM images of 4 hours reaction CdST at (a) 250 °C and (b) 260 °C.

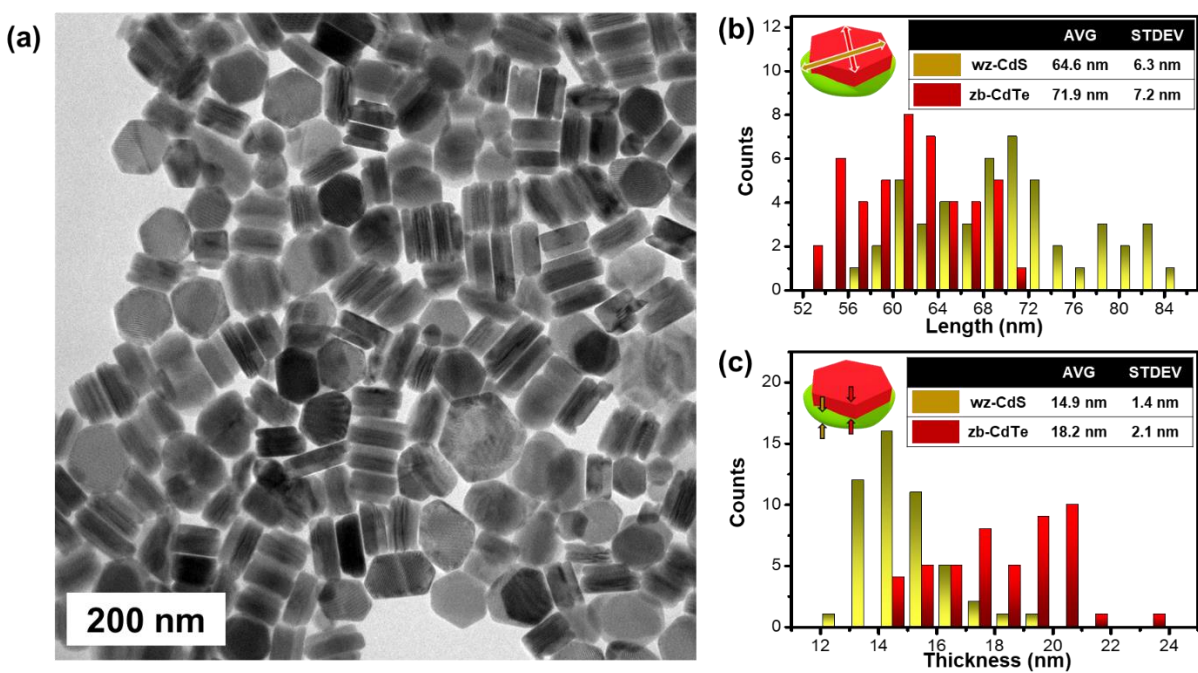


Figure S19. (a) TEM image, (b) the length, and (c) thickness distributions of thick-CdST heteronanodiscs.

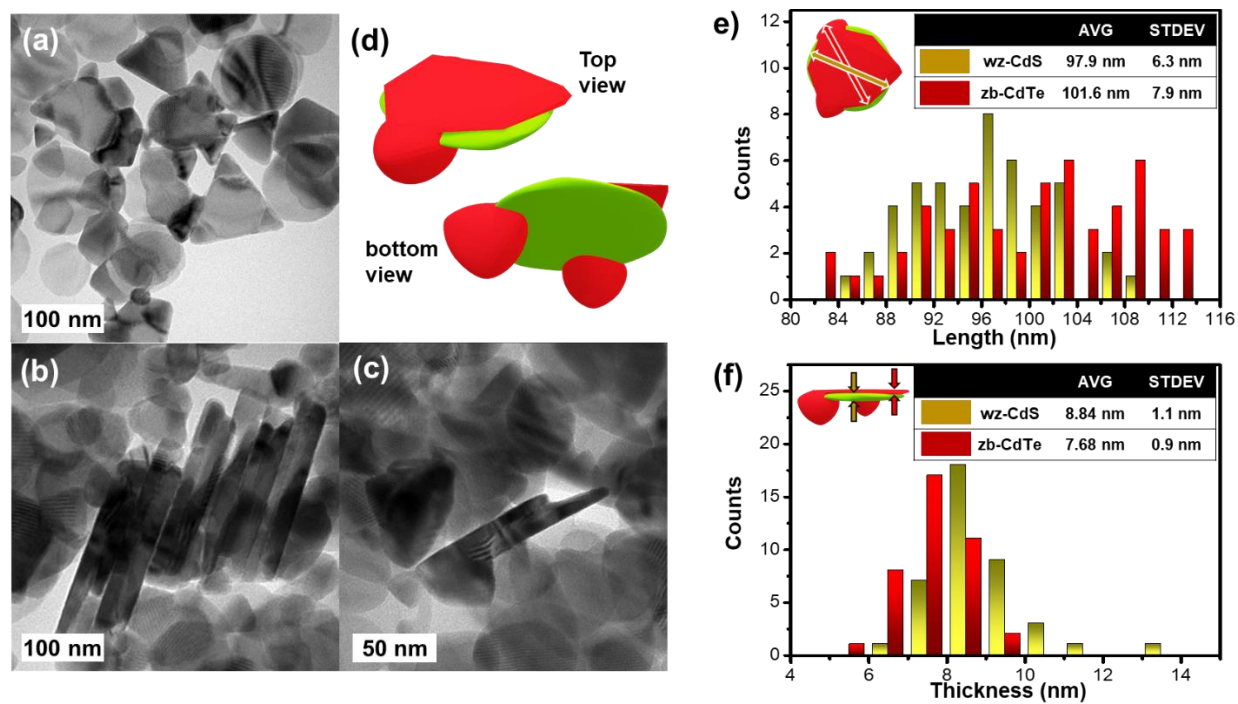


Figure S20. TEM images of thin-CdST heteronanodiscs from (a) basal plane, (b) lateral edges, and (c) intermediate at 3 h. (d) Schematic illustrations and (e) the length and (f) thickness distributions of thin-CdST heteronanodiscs.

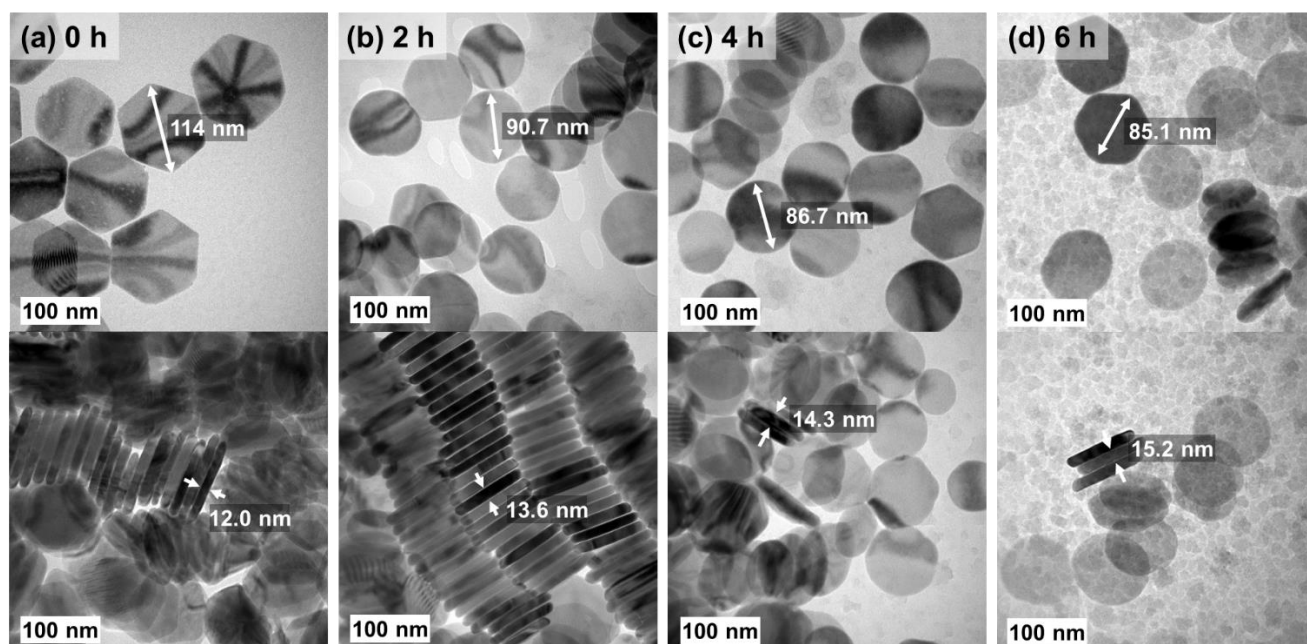


Figure S21. TEM images of intermediates with varying reaction times of CdS seeds with only TOP obtained from (a) 0 h, (b) 2 h, (c) 4 h, and (d) 6 h.

Table S1. Contents ratio of CdS ND determined by ICP-AES analysis.

Sample	Weight Percent (%)			Atomic Percent (%)		
	Cd	S	Cu	Cd	S	Cu
CdS ND	72.5 %	27.3 %	0.2 %	43.0 %	56.8 %	0.2 %

Table S2. Results of Scherrer equation analysis of s-CdST HNDs intermediates.

Reaction time	Dimensionless shape factor $K \text{ (nm)}^2$	X-ray wavelength $\lambda \text{ (Cu-K}\alpha\text{) (nm)}$	FWHM (degree)	2 theta indicated [002] plane (degree)	Calculated Thickness (nm)
0 min	0.886	0.1504	0.527	26.60	14.89
30 min			0.605	26.52	12.96
1 h			0.644	26.64	12.19
2 h			0.548	26.62	14.32
3 h			0.703	26.52	11.16
4 h			0.711	26.51	11.03

REFERENCES

- (1) Yoon, D.; Jin, H.; Ryu, S.; Park, S.; Baik, H.; Oh, S. J.; Haam, S.; Joo, C.; Lee, K., Scalable Synthesis of Djurleite Copper Sulphide ($\text{Cu}_{1.94}\text{S}$) Hexagonal Nanoplates from a Single Precursor Copper Thiocyanate and Their Photothermal Properties. *CrystEngComm* **2015**, *17*, 4627-4631.
- (2) Smilgies, D.-M. Scherrer Grain-Size Analysis Adapted to Grazing-Incidence Scattering with Area Detectors. *J.Appl. Crystallogr.* **2009**, *42*, 1030-1034